Mechanism for non-Heisenberg-exchange coupling between ferromagnetic layers

R. P. Erickson
Naval Research Laboratory, Washington, D.C. 20375

Kristl B. Hathaway and James R. Cullen
Naval Surface Warfare Center, Silver Spring, Maryland 20903

(Received 17 August 1992)

We consider a free-electron model of exchange coupling between transition-metal ferromagnetic films separated by a paramagnetic metal spacer. The minority-spin energy bands in the ferromagnets are matched to those of the paramagnetic spacer. The majority-spin electrons experience a repulsive potential arising from the lack of corresponding states in the spacer. The height of the potential barrier is equal to the exchange-energy gap in the ferromagnets. We show how the model, applicable to a trilayer film such as Fe/Cr/Fe or Co/Ru/Co, generates an infinite sum of terms with coefficients $A_{12}, B_{12}, \ldots$ in the coupling energy, extending beyond the Heisenberg-like A_{12} term of bilinear coupling between the moments of the ferromagnets. Both the A_{12} and non-Heisenberg (biquadratic) B_{12} exchange terms oscillate with spacer-layer thickness. We find that the phase of B_{12} relative to A_{12} shifts with this thickness, so that at certain regions of spacer-layer thickness, the magnitude of B_{12} is greater than that of A_{12}, and B_{12} is of the proper sign to cause 90° coupling between the ferromagnets. These special thicknesses are predicted to appear over a broad range of the ratio of Fermi to exchange-gap energies. Thus, we show from our model that biquadratic, or 90°, coupling between the ferromagnets is intrinsic to itinerant-electron exchange across the paramagnetic spacer.

I. INTRODUCTION

Early observations of exchange coupling between transition-metal magnetic layers separated by nonmagnetic metals[1–6] were striking when considered from the point of view of their bulk band structures. Both Fe/Cr and Co/Ru multilayers comprise ferromagnetic and paramagnetic elements with the same crystal structure and similar lattice constants, and in both cases the paramagnet has fewer *spd* electrons than the ferromagnet. This deficit of electrons in the paramagnet lowers its relative Fermi energy just enough to match the minority-spin bands in the ferromagnet. (See Fig. 1). Thus, when the two materials are brought together at an interface with their Fermi energies equal, the electron wave functions in the paramagnet are matched in both energy and symmetry to the minority-spin wave functions in the ferromagnet.

Subsequent observations of exchange coupling in a wide variety of transition-metal systems[7,8] has made it clear that such an exact match of band structures is not a necessary condition for exchange coupling, but the degree of band matching may play an important role in determining the strength of the coupling. The most recent observations of exchange coupling between magnetic transition metals separated by noble metals[9–12] indicates that a different kind of band matching may occur between the paramagnetic states and the ferromagnet majority-spin states.

With this condition of closely matched band structures appearing to play an important role in the coupling, it seems appropriate to model exchange-coupled systems by allowing for strong hybridization between the metals—to go beyond perturbation theory treatments such as that used to derive the Ruderman-Kittel-Kasuya-Yosida (RKKY) coupling. A nonperturbative approach to the coupling problem has also been taken by Edwards *et al.* in a calculation of the energy difference between ferromagnetically and antiferromagnetically aligned moments.[13] In addition, some early unpublished results indicated that the exchange coupling was not always of the simple Heisenberg form. Recent measurements of strong biquadratic coupling in Fe/Cr/Fe (Refs. 14 and 15) and Fe/Al/Fe [Ref. 16] systems has confirmed these early observations. It has been suggested that biquadratic coupling in the Fe/Cr/Fe systems is the result of interfacial roughness.[17]

Slonczewski[18] has recently calculated both a tunneling spin-valve (magnetoresistance) effect and an exchange coupling between transition-metal magnets separated by a thin insulating layer. He represents the magnets by free-electron spin-split bands and the insulator by a one-dimensional barrier extending above the Fermi energy in the metals. The magnitude of the calculated exchange coupling depends on the degree to which the electrons with different spins are affected by a different barrier height—the magnitude of the exchange splitting, or equivalently, the magnetic moment in the metal. Slonczewski introduces and employs a method for calculating exchange coupling from the torque produced by rotation of the magnetization of one ferromagnet relative to that of the other.

We have adapted Slonczewski's method to a model of transition-metal ferromagnet/paramagnet/ferromagnet trilayers with matched band structures appropriate for Fe/Cr as discussed above. In our model, electrons of one

ferromagnet have a finite probability of undergoing a spin flip upon transmission through the paramagnetic spacer due to the noncolinear alignment of the moments of the two ferromagnets. In particular, incident majority-spin electrons encounter a potential barrier equal to the exchange splitting of the ferromagnet bands since the paramagnetic band is matched to the minority-spin band.

In Sec. II we discuss this model and calculate the wave functions for arbitrary angle θ between the in-plane magnetizations of the ferromagnetic layers. Also, we describe how the quantum-mechanical spin-flip current is obtained from these wave functions and derive the proportionality relation between the spin-flip current and the torque on a ferromagnet layer. As a last topic in this section we show the cancellation of the nonoscillatory contributions to the spin-flip current.

In Sec. III we map our itinerant-electron model onto an empirical model of the exchange coupling between ferromagnetic layers by equating the torque (on a ferromagnetic layer) of our model to the torque implied by the phenomenological model. In this way our spin-flip current, which is expandable in a power series in $\cos\theta$, can be related to bilinear, biquadratic, and higher-order exchange terms of the empirical model. In addition to a discussion of the asymptotic forms of the bilinear and biquadratic terms, we give the results of numerical integrations of these terms for various values of the band-structure parameters. We show that the biquadratic term, which oscillates with increasing paramagnetic layer thickness, is in commensurate with the oscillations of the bilinear term. From this result we demonstrate that biquadratic, or 90°, coupling between the ferromagnetic layers is intrinsic to itinerant-electron exchange.

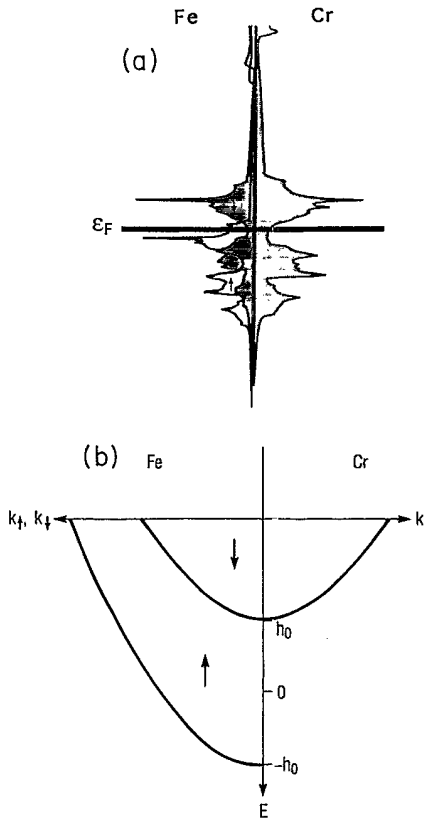

FIG. 1. (a) Density of states vs energy for majority- and minority-spin Fe *spd* bands and Cr *spd* bands, from band-structure calculations [D. A. Papaconstantopoulos, *Handbook of the Band Structure of Elemental Solids* (Plenum, New York, 1986)]. The shaded portion of the left-hand (Fe) side is the minority-spin ($\downarrow$) density of states. Fermi energy is denoted by ϵ_F. (b) Energy vs wave vector perpendicular to the interface for majority- and minority-spin Fe electrons, and Cr electrons, as used in the model discussed in the text. The value $2h_0$ is the exchange energy band gap. The minority-spin Fe and Cr bands are perfectly matched. The model should apply to other ferromagnetic/paramagnetic/ferromagnetic systems in which the minority-spin bands of the ferromagnet match the bands of the paramagnet: Co/Ru/Co, for example.

II. THE MODEL

We now proceed to a description of our free-electron model, applicable to a system such as Fe/Cr/Fe, and the method of calculating the coupling of the ferromagnets through the paramagnetic metal. Specifically, we consider a trilayer structure with perfectly smooth interfaces of total volume V consisting of two very thick ferromagnetic (Fe) layers separated by a paramagnetic (Cr) layer of variable thickness d. We assume the overall thickness of the film to be much greater than d, taking the ferromagnetic layers to be, for all intents and purposes, semi-infinite. Let y denote the direction normal to these interfaces, and let θ denote the angle between the total magnetic moments, or equivalently the axes of quantization, of the respective ferromagnets, hereafter referred to as Fe(1) and Fe(2), as in Fig. 2. The magnetic moments of both Fe layers are restricted to the plane of the film.

The electrons in Fe and Cr are treated as itinerant, with states described by plane waves. The most important feature of the band structures of these two metals for the present purpose is the similarity, both in energy and orbital symmetry, between the Cr bands and those of the minority-spin electrons of Fe. In contrast, the Fe majority states have no counterparts in Cr for energies below the bottom of the Cr band, recall Fig. 1. Thus, in consid-

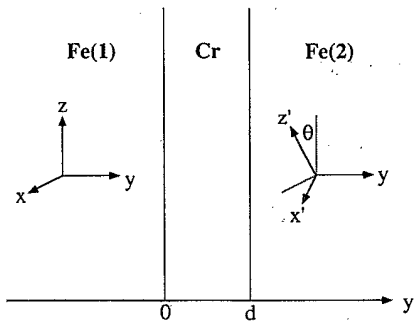

FIG. 2. The coordinate arrangement as used in the calculations described in the text. The axis of quantization of Fe(1) is z, that of Fe(2) is z', which is rotated from alignment along z by angle θ. As indicated, y is the direction perpendicular to the film plane.

ering electrons of a ferromagnet incident to the film interfaces, the minority-spin electrons of Fe are easily hybridized with those of Cr while the majority-spin electrons are confronted by an energy barrier. Our simple model therefore consists of a paramagnetic free-electron band structure for Cr and an exchange-split free-electron band structure for Fe, see Fig. 1(b), so that the barrier encountered by the majority-spin Fe electrons is equal to the exchange energy gap $2h_0$ of Fe.

The determination of the electron eigenfunctions of our model is straightforward, being similar to the elementary textbook example of a spinless particle incident to a finite potential barrier.[19] We exploit the translational symmetry parallel to the interfaces of the film, expressing an eigenfunction with spatial dependence $\mathbf{x}$ in the spinor form $\psi(\mathbf{x})=u(y)e^{i\mathbf{k}_\parallel\cdot\mathbf{x}}$, where $\mathbf{k}_\parallel$ is the component of wave vector tangent to a film interface. This leaves us with the task of evaluating the spinor $u(y)$, which varies across the thickness of the film. An expression for $u(y)$ of a majority or minority-spin electron of energy E incident at an interface, say from Fe(1), is then obtained in the Cr spacer and in the opposite Fe layer, Fe(2), by matching the function and its first derivative at the two interfaces. Matching the wave function of Fe(2) to that of Cr requires rotating the spinor of Fe(2) by angle θ to the axis of quantization of Fe(1).

The Fe layers are assumed thick enough so that an electron incident from Fe(1) is independent of one incident from Fe(2). Of course, majority and minority electrons incident from *both* Fe(1) and Fe(2) must be taken into account since every itinerant electron of our model can reside, with some finite probability, in every region of the volume V.

As an example, consider a majority (minority) plane-wave electron of energy E incident from Fe(1) whose component of wave vector along the $\hat{y}$ direction has magnitude $k_\uparrow$ ($k_\downarrow$). In the region of the paramagnetic layer $(0<y<d)$, for an incident majority-spin electron, $u^{(\uparrow)}(y)=[u_\uparrow^{(\uparrow)}(y),u_\downarrow^{(\uparrow)}(y)]$ is given by

$$u_\uparrow^{(\uparrow)}(y)=\frac{1}{\sqrt{V}}\frac{2k_\uparrow[(k_\uparrow+k_\downarrow)e^{ik_\downarrow(y-d)}-(k_\uparrow-k_\downarrow)e^{-ik_\downarrow(y-d)}\cos^2(\theta/2)]}{(k_\uparrow+k_\downarrow)^2e^{-ik_\downarrow d}-(k_\uparrow-k_\downarrow)^2e^{ik_\downarrow d}\cos^2(\theta/2)} \tag{1a}$$

and

$$u_\downarrow^{(\uparrow)}(y)=\frac{1}{\sqrt{V}}\frac{-k_\uparrow(k_\uparrow-k_\downarrow)e^{-k_\downarrow(y-d)}\sin\theta}{(k_\uparrow+k_\downarrow)^2e^{-ik_\downarrow d}-(k_\uparrow-k_\downarrow)^2e^{ik_\downarrow d}\cos^2(\theta/2)}\,. \tag{1b}$$

Similarly, in this same region, for an incident minority-spin electron we find

$$u_\uparrow^{(\downarrow)}(y)=\frac{1}{\sqrt{V}}\frac{\frac{1}{2}[(k_\uparrow-k_\downarrow)^2e^{ik_\downarrow y}-k_0^2e^{-ik_\downarrow y}]e^{ik_\downarrow d}\sin\theta}{(k_\uparrow+k_\downarrow)^2e^{-ik_\downarrow d}-(k_\uparrow-k_\downarrow)^2e^{ik_\downarrow d}\cos^2(\theta/2)} \tag{2a}$$

and

$$u_\downarrow^{(\downarrow)}(y)=\frac{1}{\sqrt{V}}\frac{e^{ik_\downarrow(y-d)}-k_0^2e^{-ik_\downarrow(y-d)}\sin^2(\theta/2)}{(k_\uparrow+k_\downarrow)^2e^{-ik_\downarrow d}-(k_\uparrow-k_\downarrow)^2e^{ik_\downarrow d}\cos^2(\theta/2)}\,, \tag{2b}$$

where $k_0^2\equiv k_\uparrow^2-k_\downarrow^2=4mh_0/\hbar^2$. Here, of course, m is the mass of an electron and $\hbar$ is Planck's constant.

A. The spin-flip current and the equation of torque

Our model interprets the interaction between the ferromagnetic layers Fe(1) and Fe(2) in terms of a simple electron exchange. An electron of a majority- or minority-spin state, incident from one ferromagnet, is transmitted through the paramagnetic layer to the other ferromagnet with a finite probability of undergoing a spin-flip due to the oblique alignment of the moments of the respective ferromagnets. The probability of a spin flip varies continuously from zero, in the ferromagnetic state of the film ($\theta=0$), to a maximum value in the antiferromagnetic state ($\theta=\pi$).

Following Slonczewski,[18] we determine the torque induced on one ferromagnetic layer, Fe(1), by the other, Fe(2). Slonczewski's method of calculating the torque involves the construction of a spin-flip or exchange current, which is a measure of the probability that an incident electron will undergo a change of spin state on transmission through the paramagnetic spacer. It is analogous in form to the probability current of a spinless particle,[20] and appears in descriptions of itinerant ferromagnetism.[21]

For the remainder of this section we briefly discuss the formulation of the spin current and its relation to the torque on a ferromagnet.

One begins by defining a spin-density vector

$$\rho(\mathbf{x},t)=\psi^\dagger(\mathbf{x},t)\sigma\psi(\mathbf{x},t)\,, \tag{3}$$

where σ is the vector of Pauli matrices. Letting $\mathbf{S}=(\hbar/2)\sigma$ be the spin of an electron of a given ferromagnetic layer, the meaning of Eq. (3) becomes clear from the expectation value of $\mathbf{S}(t)$, viz.,

$$\langle \mathbf{S}(t)\rangle = \int dV\, \psi^{\dagger}(\mathbf{x},t)\mathbf{S}\psi(x,t) = \frac{\hbar}{2}\int dV\, \rho(\mathbf{x},t)\ , \tag{4}$$

where the integral encloses the volume of the given ferromagnet. Then, examining $\partial\langle \mathbf{S}(t)\rangle/\partial t$, and therefore $\partial\rho(\mathbf{x},t)/\partial t$, we are led to define a current tensor $\mathbf{j}(\mathbf{x},t)$, with Cartesian components given by

$$j_{\alpha\beta}(\mathbf{x},t)=\frac{\hbar}{2im}\left[\psi^{\dagger}(\mathbf{x},t)\sigma_{\beta}\frac{\partial\psi(\mathbf{x},t)}{\partial x_{\alpha}} - \left[\frac{\partial\psi^{\dagger}(\mathbf{x},t)}{\partial x_{\alpha}}\right]\sigma_{\beta}\psi(\mathbf{x},t)\right], \tag{5a}$$

which satisfies a continuity equation involving $\rho(\mathbf{x},t)$:[20]

$$\frac{\partial\rho(\mathbf{x},t)}{\partial t}+\nabla\cdot\mathbf{j}(\mathbf{x},t)=0\ . \tag{5b}$$

Equation (5a) is valid in the absence of spin-orbit coupling.

We can apply this idea to our trilayer film, which has Fe/Cr interfaces of area A parallel to the x-z plane, recall Fig. 2. Thus, for a given electron of spin $\mathbf{S}$ in the volume V_1 of Fe(1), we find the time rate of change of the expectation value of the relevant y component of this spin to be

$$\frac{\partial\langle S_y(t)\rangle}{\partial t}=-\frac{\hbar}{2}\int_{V_1}dV\,\nabla\cdot\mathbf{j}(\mathbf{x},t)\cdot\hat{y} =-\frac{\hbar}{2}\int_{A}dA\, j_{yy}(\mathbf{x},t)\big|_{y=0^+} =-\frac{\hbar}{2}A j_{yy}(y)\big|_{y=0^+}\ . \tag{6a}$$

From Eq. (5a), the current $j_{yy}|_{y=0^+}$, uniform throughout the paramagnetic layer, is

$$j_{yy}\big|_{y=0^+}=\frac{\hbar}{m}\mathrm{Re}\left[u_{\downarrow}(y)^*\frac{\partial u_{\uparrow}(y)}{\partial y} - \left[\frac{\partial u_{\downarrow}(y)^*}{\partial y}\right]u_{\uparrow}(y)\right]. \tag{6b}$$

Now, defining $\mathbf{S}_1$ as the *total* spin of Fe(1), we can determine $\partial\langle S_{1,y}(t)\rangle/\partial t$ by summing over all electron states up to the Fermi energy in Eqs. (6), including those of majority and minority electrons incident from *both* Fe(1) and Fe(2). In this way, summing the spin-flip currents of the form of Eq. (6b) and labeling the net current as j_T, we have from Eqs. (6)

$$\frac{\partial\langle S_{1,y}(t)\rangle}{\partial t}=-\tfrac{1}{2}A\hbar j_T\ . \tag{7}$$

Equation (7) then implies that the torque on Fe(1) can be determined by evaluating the net spin-flip current j_T in the paramagnet.

We give a brief synopsis of how j_T of our model is evaluated. The spin-flip current due to a majority-spin electron of energy E incident from Fe(1) is obtained by applying Eqs. (1) to Eq. (6b); call this current $j_e^{(\uparrow)}$. In our model, which exactly matches the Cr band to the Fe minority-spin band, one finds $j_e^{(\uparrow)}$ to be zero for $E>h_0$. Similarly, one obtains the current due to a minority-spin electron incident from Fe(1) by applying Eqs. (2) to Eq. (6b); call this current $j_e^{(\downarrow)}$. Note, $j_e^{(\downarrow)}$ exists strictly for energies $E>h_0$ by definition of a minority-spin electron. The net current of majority- and minority-spin electrons j_T is calculated by summing both $j_e^{(\uparrow)}$ and $j_e^{(\downarrow)}$ over allowed states up to their respective Fermi energies, then multiplying by a factor of 2 to account for electrons incident from Fe(2), which contribute equally to the total spin current.

In this way, summing over allowed states $\mathbf{k}=(\mathbf{k}_{\parallel},k_{\uparrow})$ and letting $k_F^{(\uparrow)}$ be the Fermi wave number of the majority band of Fe, we find the net majority-spin current $j^{(\uparrow)}$ to be

$$j^{(\uparrow)}=2\sum_{0<k_{\uparrow}<k_0}j_e^{(\uparrow)}=-\frac{\hbar}{2\pi^2 m}\int_0^{k_0}dk_{\uparrow}\int_0^{\sqrt{k_F^{(\uparrow)2}-k_{\uparrow}^2}}k_{\parallel}dk_{\parallel}\frac{4\kappa k_{\uparrow}^2(\kappa^2-k_{\uparrow}^2)e^{-2\kappa d}\sin\theta}{|(k_{\uparrow}+i\kappa)^2-(k_{\uparrow}-i\kappa)^2e^{-2\kappa d}\cos^2(\theta/2)|^2}\ , \tag{8a}$$

where $\kappa\equiv ik_{\downarrow}=\sqrt{k_0^2-k_{\uparrow}^2}$. Similarly, summing over states $\mathbf{k}=(\mathbf{k}_{\parallel},k_{\downarrow})$ and letting $k_F^{(\downarrow)}$ be the Fermi wave number of the minority band of Fe, the net minority-spin current $j^{(\downarrow)}$ is

$$j^{(\downarrow)}=2\sum_{0<k_{\downarrow}<k_F^{(\downarrow)}}j_e^{(\downarrow)} =-\frac{\hbar}{2\pi^2 m}\int_0^{\sqrt{k_F^{(\downarrow)2}-k_{\downarrow}^2}}k_{\parallel}dk_{\parallel}\frac{k_{\downarrow}k_0^4\sin(2k_{\downarrow}d)\sin\theta}{|(k_{\uparrow}+k_{\downarrow})^2-(k_{\uparrow}-k_{\downarrow})^2e^{2ik_{\downarrow}d}\cos^2(\theta/2)|^2}\ , \tag{8b}$$

where $k_{\uparrow}=\sqrt{k_0^2+k_{\downarrow}^2}$. Thus, the net current j_T is then

$$j_T=j^{(\uparrow)}+j^{(\downarrow)}\ , \tag{9}$$

which determines the torque on Fe(1) when Eq. (9) is substituted into Eq. (7).

B. The cancellation of nonoscillatory terms of the spin-flip current

In the previous subsection we derived the means by which the spin-flip current of our model can be evalu-

ated. However, our task is not yet finished. In fact, the form of the spin-flip current as given by Eqs. (8) and (9) has led us to an interesting point which must be addressed before any practical calculation can be considered.

The point concerns the following. Many years ago, Bardasis *et al.*[22] considered the effect of a nonferromagnetic electron gas in contact with a ferromagnetic one. They found the excess spin density established in the nonferromagnetic (and ferromagnetic) electron gas to be entirely of the RKKY oscillatory type, contributed by electrons of energy greater than the Fermi energy of the nonferromagnetic metal. The evanescent slowly varying components of this spin density are exactly canceled by the contribution from electrons of energy less than the Fermi energy. In fact, when the exchange potential between the ferromagnetic and nonferromagnetic metals is weak enough to be treated by perturbation theory, they found a result precisely that of RKKY theory. They showed this result to be quite general, owing to the closure property of the eigenstates of the system.

The generality of the result of Bardasis *et al.* implies that our model must also exhibit this cancellation property. In fact, we show that the minority spin-flip current $j^{(\downarrow)}$ exactly cancels the nonoscillatory part of $j^{(\uparrow)}$ in Eq. (9).

To see this, consider $j^{(\downarrow)}$ as given in Eq. (8b). After integration with respect to $k_{\parallel}$ and a change of variable $z=k_{\downarrow}/k_0$, we may write

$$j^{(\downarrow)}=\frac{\hbar k_0^4}{4\pi^2 m}\int_0^{z_F} dz \frac{z(z-\sqrt{1+z^2})^4(z^2-z_F^2)\sin(2k_0 dz)\sin\theta}{1-2(z-\sqrt{1+z^2})^4\cos(2k_0 dz)\cos^2(\theta/2)+(z-\sqrt{1+z^2})^8\cos^4(\theta/2)}, \tag{10}$$

where $z_F\equiv k_F^{(\downarrow)}/k_0$. In the Appendix, we show how $j^{(\uparrow)}$ of Eq. (8a) can be written as an integral over an interval from zero to infinity with integrand of the same magnitude as that of Eq. (10), but opposite in sign. Thus, comparing Eq. (A15) with Eq. (10) we immediately see the cancellation which must occur in the expression of the spin-flip current j_T of Eq. (9). Hence, we have

$$j_T=-\frac{\hbar k_0^4}{4\pi^2 m}\int_{z_F}^{\infty} dz \frac{z(z-\sqrt{1+z^2})(z^2-z_F^2)\sin(2k_0 dz)\sin\theta}{1-2(z-\sqrt{1+z^2})^4\cos(2k_0 dz)\cos^2(\theta/2)+(z-\sqrt{1+z^2})^8\cos^4(\theta/2)}. \tag{11}$$

Equation (11) was previously evaluated in the vicinity of $\theta=\pi$, for the special case of antiferromagnetically coupled layers.[23] In the next section we discuss the oscillatory character of j_T as given by Eq. (11), and we relate it, via the torque implied by Eq. (7), to a model of the interacting ferromagnetic layers.

III. RESULTS AND DISCUSSION

As we have mentioned in the Introduction, there has been considerable investigation of the coupling of thin ferromagnetic layers separated by nonferromagnetic interlayers.[1-12] In particular, in addition to the observed ferromagnetic-antiferromagnetic oscillatory exchange coupling, there is evidence of 90°, or *biquadratic,* coupling in Fe/Cr/Fe films. Most notably in Fe/Cr/Fe wedges, by means of Kerr magneto-optic microscopy,[14] domains on either side of the Cr spacer have been observed oriented at 90°. The 90° orientation has been detected along the wedge at critical values of the Cr thickness corresponding to transitions between ferromagnetically and antiferromagnetically aligned domains. Similar evidence has been found in micrographs made using scanning-electron microscopy with polarization analysis.[15]

From the analysis of Rührig of Ref. 14, the energy of exchange coupling between the Fe layers can be written phenomenologically as

$$E_c=A_{12}(1-\mathbf{m}_1\cdot\mathbf{m}_2)+\tfrac{1}{2}B_{12}[1-(\mathbf{m}_1\cdot\mathbf{m}_2)^2], \tag{12a}$$

where $\mathbf{m}_1$ and $\mathbf{m}_2$ are the unit moments of Fe(1) and Fe(2), respectively. Additionally, with $\mathbf{m}_1\cdot\mathbf{m}_2=\cos\theta$, Eq. (12a) implies a torque proportional to

$$\frac{\partial E_c}{\partial\theta}=(A_{12}+B_{12}\cos\theta)\sin\theta. \tag{12b}$$

The bilinear coefficient A_{12} defines the strength and character (ferromagnetic-antiferromagnetic) of the oscillatory Heisenberg-like coupling. The biquadratic coefficient B_{12} generates 90° coupling between $\mathbf{m}_1$ and $\mathbf{m}_2$, or more precisely a noncolinear state $\cos\theta=A_{12}/|B_{12}|$, when $B_{12}<-|A_{12}|$, a criterion which is favorable when A_{12} approaches zero, the transition between ferromagnetically and antiferromagnetically coupled moments.

From the standpoint of theory, as much as the bilinear term of Eqs. (12) is of interest, the existence of a biquadratic term is even more so since it obviously compounds the problem of addressing the fundamental nature of the overall coupling mechanism of the ferromagnetic films. The authors of Ref. 14 have suggested two possible interpretations of the biquadratic term of Eqs. (12): one being that the biquadratic term is a natural continuation of a Heisenberg spin Hamiltonian to higher orders while the other interpretation is that the biquadratic term is a second-order Dzyaloshinski term. Recently, Slonczewski has proposed that the biquadratic term is a result of spatial fluctuations of the Cr thickness, indicative of steplike terraces at the Fe/Cr interfaces.[17]

Here, we equate the torque on the ferromagnet Fe(1), as given by our free-electron model, to that implied by Eq. (12b). Specifically, equating Eq. (7) to Eq. (12b) we have

$$-\tfrac{1}{2}A\hbar j_T=(A_{12}+B_{12}\cos\theta)\sin\theta\ , \tag{13}$$

where j_T is given by Eq. (11). In fact j_T, or more precisely the integrand of Eq. (11), can be expanded about $\cos\theta=0$ in an analytic sum involving powers of $\cos\theta$. This determines A_{12} and B_{12} within the context of our model and realizes an infinite series of terms in ascending powers of $\mathbf{m}_1\cdot\mathbf{m}_2$ in Eq. (12a). Thus, for example, in expanding j_T we establish the definitions

$$A_{12}=\frac{A\hbar^2k_0^4}{8\pi^2m}\int_{z_F}^{\infty}dz\frac{z(z-\sqrt{1+z^2})^4(z^2-z_F^2)\sin(2k_0dz)}{1-(z-\sqrt{1+z^2})^4\cos(2k_0dz)+(1/4)(z-\sqrt{1+z^2})^8} \tag{14a}$$

and

$$B_{12}=\frac{A\hbar^2k_0^4}{8\pi^2m}\int_{z_F}^{\infty}dz\frac{z(z-\sqrt{1+z^2})^8[\cos(2k_0dz)-(1/2)(z-\sqrt{1+z^2})^4](z^2-z_F^2)\sin(2k_0dz)}{[1-(z-\sqrt{1+z^2})^4\cos(2k_0dz)+(1/4)(z-\sqrt{1+z^2})^8]^2}\ . \tag{14b}$$

Higher-order coefficients of the expansion can be defined, although we will not state them explicitly here. Equations (14) indicate that the overall amplitude of B_{12} is smaller than that of A_{12} since the integrand of B_{12} contains $(z-\sqrt{1+z^2})^4$ to second order. In fact, as can be demonstrated, higher-order coefficients contain $(z-\sqrt{1+z^2})^4$ to ever-increasing power so that the amplitude of each successive coefficient in the expansion $A_{12},B_{12},\ldots$ is smaller than the amplitude of the previous coefficient. For our purposes here, it will suffice to consider Eqs. (14) only, particularly as functions of the Cr thickness d.

Before we consider Eqs. (14) in detail, we examine their forms in the limits of $d=0$ and $d\to\infty$, which are especially revealing.

The precise expansion of j_T of Eq. (11), which defines $A_{12},B_{12},\ldots$ in our model, can be written

$$j_T=\sum_{n=0}^{\infty}j_n\cos^n\theta\sin\theta\ , \tag{15a}$$

where the j_n are given by

$$j_n=-\frac{\hbar k_0^4}{4\pi^2m}\sum_{l=n}^{\infty}\begin{bmatrix}l\\n\end{bmatrix}\left[\frac{1}{2}\right]^l\int_{z_F}^{\infty}dz\,z(z^2-z_F^2)(z-\sqrt{1+z^2})^{4(l+1)}\sin[2(l+1)k_0dz]\ . \tag{15b}$$

One can show from Eq. (15b), by writing the sum over l in closed form, that $A_{12}=-(A\hbar/2)j_0$ and $B_{12}=-(A\hbar/2)j_1$ are identical to Eqs. (14).

In the limit of $d=0$, with $z_F=k_F^{(1)}/k_0$ held fixed, where again, $k_0^2=k_F^{(\uparrow)^2}-k_F^{(\downarrow)^2}=4mh_0/\hbar^2$, the integrals of the sum in Eq. (15b) vanish except for the case $l=0$, which implies

$$\lim_{d\to0}j_n=-\frac{\hbar k_0^4}{4\pi^2m}\frac{\pi}{32}\delta_{n,0}\ . \tag{16}$$

Therefore, in the limit $d=0$, A_{12} attains the value

$$A_{12}^{(0)}\equiv\lim_{d\to0}A_{12}=\frac{A\hbar^2k_0^4}{256\pi m}\ , \tag{17}$$

while B_{12}, and all higher-order coefficients, vanish. Thus, ferromagnetic Heisenberg-like coupling, with energy proportional to $A_{12}^{(0)}>0$, is the only coupling in the limit $d\to0$, and A_{12} always begins, as a function of d, with this same initial ferromagnetic phase, regardless of the coupling strength k_0.

In the limit $2k_F^{(\downarrow)}d\to\infty$, with $z_F=k_F^{(\downarrow)}/k_0$ held fixed, the integral of Eq. (15b) can be integrated by parts to obtain

$$j_n=\frac{\hbar k_F^{(\downarrow)^4}}{2\pi^2m}\sum_{l=n}^{\infty}\begin{bmatrix}l\\n\end{bmatrix}\left[\frac{1}{2}\right]^l\Big/(l+1)^{-2}\left[\frac{k_F^{(\uparrow)}-k_F^{(\downarrow)}}{k_F^{(\uparrow)}+k_F^{(\downarrow)}}\right]^{2(l+1)}\frac{\sin[(l+1)k_F^{(\downarrow)}d]}{(2k_F^{(\downarrow)}d)^2}+O[(2k_F^{(\downarrow)}d)^{-3}]\ . \tag{18}$$

In the weak-coupling limit, $k_F^{(\uparrow)}\cong k_F^{(\downarrow)}$, the first term in the sum over l of Eq. (18) suffices, and we have

$$A_{12}=-\tfrac{1}{2}A\hbar j_0\cong-\frac{A\hbar^2k_F^{(\downarrow)^2}}{16\pi^2m}[k_F^{(\uparrow)}-k_F^{(\downarrow)}]^2\frac{\sin(2k_F^{(\downarrow)}d)}{(2k_F^{(\downarrow)}d)^2}\ , \tag{19}$$

$$k_F^{(\uparrow)}\cong k_F^{(\downarrow)}\ ,$$

while B_{12} and all higher-order coefficients are negligible; Eq. (19) is precisely the RKKY result, attributable to the A_{12} term only. In fact, the sum over l in Eq. (18), which is always convergent, illustrates well the departure of the asymptotic coupling oscillations from the RKKY theory as the coupling strength increases. Thus, with increasing coupling strength, higher harmonics in l become more important.

We now turn to a more general discussion of A_{12} and B_{12}. In Fig. 3(a), we plot the results of numerical calculations of A_{12} of Eq. (14a) as a function of $2k_F^{(\downarrow)}d$ for several values of $z_F=k_F^{(\downarrow)}/k_0$. Similarly, in Fig. 3(b), we plot the results of numerical calculations of B_{12} of Eq. (14b) as a function of $2k_F^{(\downarrow)}d$. All curves are normalized by a factor $A_{12}^{(0)}$, a function of the coupling strength as given in Eq. (17), so care must be taken in comparing the overall amplitudes of the curves of a given plot frame since each curve of the plot frame is normalized differently. All curves in Fig. 3(a) rise to the value of unity as $2k_F^{(\downarrow)}d\to 0$ while all curves of Fig. 3(b) approach zero in this same limit. In Fig. 3(b), the curves corresponding to $z_F=0.2$ and 0.5 have absolute maxima which occur off the scale of the plot. These maxima are $B_{12}\cong 0.0034A_{12}^{(0)}$ at $2k_F^{(\downarrow)}d\cong 0.2$ for $z_F=0.2$ and $B_{12}\cong 0.0015A_{12}^{(0)}$ at $2k_F^{(\downarrow)}d\cong 0.3$ for $z_F=0.5$.

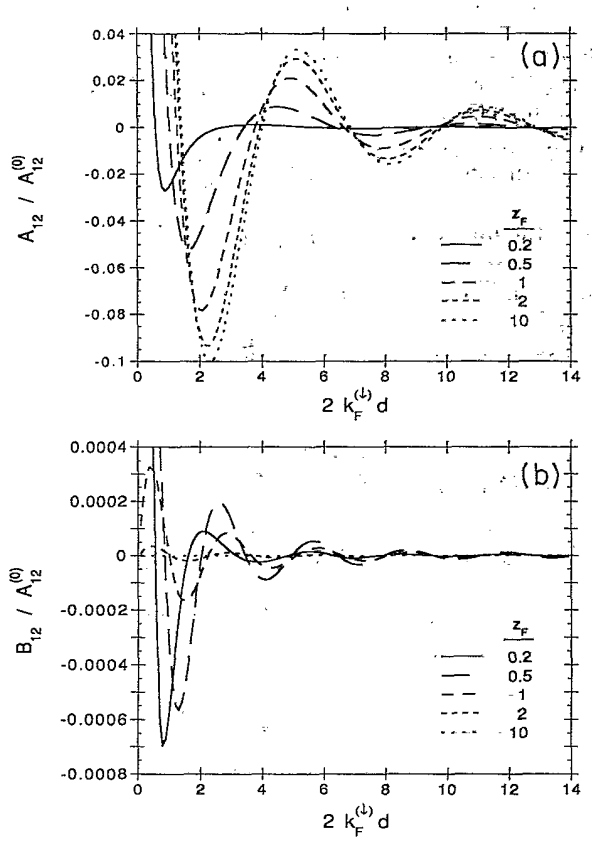

FIG. 3. The strength of the exchange-coupling energy as a function of paramagnetic spacer thickness d, in units of $2k_F^{(\downarrow)}d$ where $k_F^{(\downarrow)}$ is the Fermi wave number of the electrons of the paramagnet. Here, $z_F=k_F^{(\downarrow)}/k_0$, where k_0 is proportional to the square root of the ferromagnetic exchange splitting. Both sets of curves are normalized to the Heisenberg-like $d=0$ exchange energy $A_{12}^{(0)}$, which is proportional to k_0^4. Because of the choice of normalization, the peaks in the strong-coupling curves of A_{12} for $d\neq 0$ appear to be smaller than the weak-coupling ones, although they are actually larger on an absolute scale. (a) Heisenberg-like exchange energy A_{12}. Note the shift in the first antiferromagnetic ($A_{12}<0$) peak to smaller d with increasing strength of the ferromagnetic exchange splitting (smaller z_F). (b) The lowest-order (in $\mathbf{m}_1\cdot\mathbf{m}_2$), non-Heisenberg-like exchange energy B_{12}. The curves corresponding to $z_F=0.2$ and 0.5 have absolute maxima which occur off the scale of the plot. These maxima are $B_{12}\cong 0.0034A_{12}^{(0)}$ at $2k_F^{(\downarrow)}d\cong 0.2$ for $z_F=0.2$ and $B_{12}\cong 0.0015A_{12}^{(0)}$ at $2k_F^{(\downarrow)}d\cong 0.3$ for $z_F=0.5$. All curves approach zero as $d\to 0$.

As we mentioned in the paragraph following Eqs. (14), the overall amplitude of A_{12} is greater than that of B_{12} as a function of $2k_F^{(\downarrow)}d$, as is evident from Fig. 3. As a comparison of the relative strengths of the A_{12} and B_{12} coefficients, we consider the ratio of the first antiferromagnetic peak of A_{12} ($A_{12}<0$) to the first maximum of B_{12}. For example, from our numerical calculations, for $z_F=2.0$, 1.0, 0.5, and 0.2, this ratio is approximately 2300, 240, 35, and 8, respectively. Thus, as the coupling strength increases (z_F decreases), the amplitude of B_{12} increases toward that of A_{12}.

While the overall amplitude of B_{12} is generally smaller than that of A_{12}, the striking result upon comparing A_{12} and B_{12} of Fig. 3, is that, in general, A_{12} and B_{12} of a given z_F oscillate out of phase as a function of $2k_F^{(\downarrow)}d$. In fact, the phase slip between A_{12} and B_{12} is a function of $2k_F^{(\downarrow)}d$ and z_F, in particular, decreasing as $2k_F^{(\downarrow)}d\to\infty$. The fact that the phase slip vanishes in the asymptotic limit of large $2k_F^{(\downarrow)}d$ is apparent from Eq. (18), where the nodes $2k_F^{(\downarrow)}d=\pi n$ (integer $n\gg 1$) of $A_{12}=-(A\hbar/2)j_0$ coincide with the nodes of $B_{12}=-(A\hbar/2)j_1$. As implied by the $d=0$ forms of A_{12} and B_{12} [$A_{12}^{(0)}$ of Eq. (17) and zero, respectively], the phase slip is largest for small $2k_F^{(\downarrow)}d$.

In Fig. 4 we plot B_{12} and nodes of A_{12}, indicated by the arrows and labeled with integers, for three values of z_F. The panel of figures in Fig. 4 illustrate the phase slip between A_{12} and B_{12} as the coupling strength is varied. The effect is most pronounced at small values of $2k_F^{(\downarrow)}d$ where the amplitude of B_{12} is greatest. In particular, if attention is fixed on the node of A_{12} labeled by the number "3," we see that B_{12}, initially greater than zero at node "3" [Fig. 4(a)], slips past the node with decreasing coupling strength (increasing z_F), becoming negative at the node [Fig. 4(c)]. Note, node "3" of A_{13} itself shifts to larger $2k_F^{(\downarrow)}d$ as the coupling strength decreases (z_F increases).

If the criterion for biquadratic coupling $B_{12}<-|A_{12}|$, corresponding to the energy E_c of Eq. (12a), is now considered, then it is apparent from Fig. 4 that the intrinsic phase difference between the A_{12} and B_{12} coefficients of our model can give rise to this kind of coupling between the ferromagnetic layers. Thus, for example, in Fig. 4(a), in the vicinity of node "1" of A_{12}, corresponding to a critical spacer thickness $2k_F^{(\downarrow)}d\cong 0.8$, $B_{12}<0$ implies 90° coupling, but there is no 90° coupling at nodes "2"–"5" where $B_{12}>0$. As z_F increases, Fig. 4(b) illustrates the appearance of 90° coupling at node "2" while Fig. 4(c) shows the onset of 90° coupling at node "3" (and possibly node "4"), in addition to nodes "1" and "2."

Thus, as the coupling strength or exchange splitting of the ferromagnetic energy bands decreases (z_F increases), the biquadratic state of 90° arrangement of ferromagnetic moments appears, with increasing $2k_F^{(\downarrow)}d$, at successive

nodes of A_{12}, as depicted in Fig. 4. However, for a given z_F, as $2k_F^{(\downarrow)}d \to \infty$, the nodes of A_{12} and B_{12} eventually coincide, as we demonstrated from Eq. (18), so the effect is restricted to a finite number of initial A_{12} nodes.

IV. CONCLUSION

From the foregoing, we see that a model of mismatched majority-spin electrons and matched minority-spin electrons treated as a finite-barrier tunneling problem leads to oscillatory biquadratic, as well as bilinear, exchange coupling between ferromagnetic films. Moreover, the biquadratic coupling dominates the bilinear coupling for critical values of spacer thickness, over a range of coupling strengths, implying the existence of 90° relative spin orientations in the ferromagnets at these thicknesses. This model, being free-electron-like, fails to produce the doubly periodic oscillations seen in many of the trilayer and multilayer experiments. It is therefore not possible to make more detailed comparisons between the experimental results and our model. There may be several sources of biquadratic coupling; our results nevertheless make clear that biquadratic coupling is a feature intrinsic to exchange-coupled films.

ACKNOWLEDGMENTS

R.P.E. was supported by the National Research Council and the Naval Research Laboratory. This work has also been supported by NSWC and by the Office of Naval Research.

APPENDIX

Here, we show how the current $j^{(\downarrow)}$ can be made to cancel with part of $j^{(\uparrow)}$. The procedure is similar in spirit to that presented in Ref. 22, but complicated by the presence of a denominator in the integrand of $j^{(\uparrow)}$.

We can express the majority spin-flip current of Eq. (8a) in the form of the minority spin-flip current of Eq. (10). After integration with respect to $k_{\parallel}$ and change of variable $z_\uparrow = k_\uparrow / k_0$, Eq. (8a) becomes

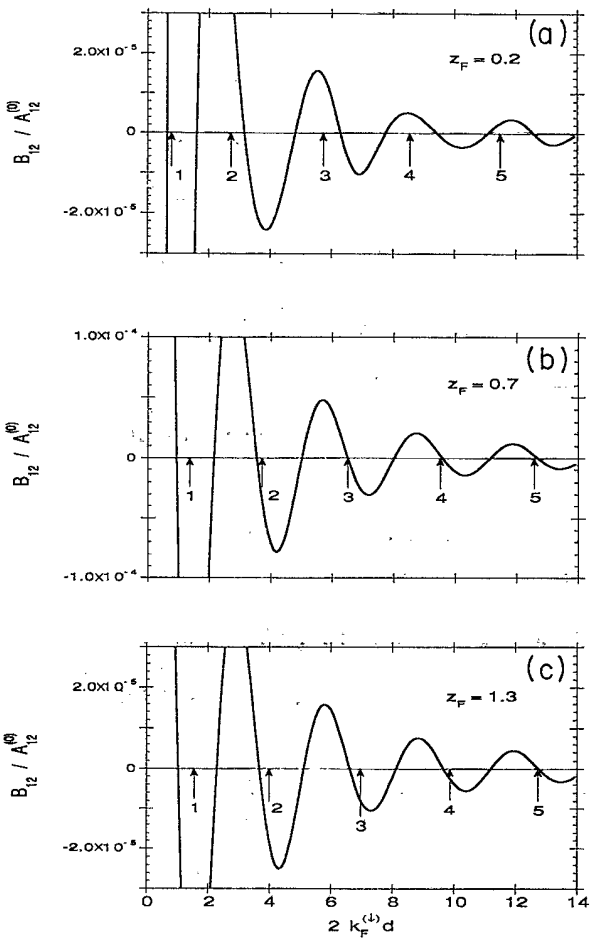

FIG. 4. Plots of B_{12} vs $2k_F^{(\downarrow)}d$ with the zeros (nodes) of A_{12} marked by arrows. (a)–(c) illustrate the effect that the coupling strength has on the relative phases of the A_{12} and B_{12} oscillations. In (a), corresponding to $z_F = 0.2$, only for d close to node "1" can there be 90° coupling ($B_{12} < 0$ when $A_{12} \cong 0$); in (b), corresponding to $z_F = 0.7$, the region near node "2" is now also representative of 90° coupling; and in (c), corresponding to $z_F = 1.3$, enough slippage has occurred that regions of d near nodes "1", "2", and "3" have B_{12} clearly negative.

$$j^{(\uparrow)} = -\frac{\hbar k_0^4}{4\pi^2 m}\int_0^1 dz_\uparrow \frac{4zz_\uparrow^2(z^2-z_\uparrow^2)(z^2+z_F^2)e^{-2k_0 dz}\sin\theta}{|(z_\uparrow+iz)^2-(z_\uparrow-iz)^2 e^{-2k_0 dz}\cos^2(\theta/2)|^2}, \tag{A1}$$

where $z \equiv \sqrt{1-z_\uparrow^2}$ and we have used $(k_F^{(\uparrow)}/k_0)^2 = 1+z_F^2$. Then, changing the variable of integration from $z_\uparrow$ to z where $zdz = -z_\uparrow dz_\uparrow$, we may write the equivalent expression

$$j^{(\uparrow)} = -\frac{\hbar k_0^4}{4\pi^2 m}\int_0^1 dz \frac{4z_\uparrow z^2(z^2-z_\uparrow^2)(z^2+z_F^2)e^{-2k_0 dz}\sin\theta}{|(z-iz_\uparrow)^2-(z+iz_\uparrow)^2 e^{-2k_0 dz}\cos(\theta/2)|^2}, \tag{A2}$$

with $z_\uparrow = \sqrt{1-z^2}$ a positive number on the interval $0 < z < 1$.

Now, it is possible to express the integrand of $j^{(\uparrow)}$ as the imaginary part of a complex number. Noting $|z+iz_\uparrow|^2 = z^2+z_\uparrow^2 = 1$, it is easy to verify that

$$j^{(\uparrow)} = -\frac{\hbar k_0^4}{4\pi^2 m}\frac{\sin\theta}{\cos^2(\theta/2)}\int_0^1 dz\ \mathrm{Im}\left[\frac{z(z^2+z_F^2)}{1-(z+iz_\uparrow)^4 e^{-2k_0 dz}\cos^2(\theta/2)}\right] \tag{A3}$$

is the same as Eq. (A2).

Let us digress for a moment and consider the function

$$f(z)=1-(z+iz_{\uparrow})^4 e^{-2k_0 dz}\cos^2\frac{\theta}{2} . \tag{A4a}$$

When $z>1$ we have $z_{\uparrow}=i\sqrt{z^2-1}$ so that

$$f(z)=1-(z-\sqrt{z^2-1})^4 e^{-2k_0 dz}\cos^2\frac{\theta}{2},\quad z\geq 1 . \tag{A4b}$$

Note, $z-\sqrt{z^2-1}\leq 1$ and $\exp(-2k_0 dz)\cos^2(\theta/2)<1$ when $z\geq 1$, which means

$$(z-\sqrt{z^2-1})^4 e^{-2k_0 dz}\cos^2\frac{\theta}{2}<1,\quad z\geq 1 \tag{A5}$$

so that $f(z)>0$ when $z\geq 1$.

We have thus shown that the integrand of Eq. (A3) is analytic for $z\geq 1$. Additionally, the integrand of Eq. (A3) is zero for $z\geq 1$ since $f(z)$ of Eq. (A4b) is real. We are therefore allowed to extend the integral of Eq. (A3) to infinity:

$$j^{(\uparrow)}=-\frac{\hbar k_0^4}{4\pi^2 m}\frac{\sin\theta}{\cos^2(\theta/2)}\int_0^{\infty} dz\ \mathrm{Im}\left[\frac{z(z^2+z_F^2)}{1-(z+iz_{\uparrow})^4 e^{-2k_0 dz}\cos^2(\theta/2)}\right] . \tag{A6}$$

Note, the integrand of Eq. (A6) is the imaginary part of a complex number whose real part is unbounded as $z\to\infty$, so we must be careful in what follows. Let us define the integral

$$I(\alpha)=\int_0^{\infty} dz\frac{z(z^2+z_F^2)e^{-\alpha z}}{1-(z+i\sqrt{1-z^2})^4 e^{-2k_0 dz}\cos^2(\theta/2)},\quad 0<\arg\alpha<\frac{\pi}{2} \tag{A7}$$

and write

$$j^{(\uparrow)}=-\frac{\hbar k_0^4}{4\pi^2 m}\frac{\sin\theta}{\cos^2(\theta/2)}\lim_{\alpha\to 0}\mathrm{Im}I(\alpha) . \tag{A8}$$

For reasons that will become apparent, change the variable of integration in Eq. (A7) so that the integral corresponds to a path over the positive imaginary axis, i.e., let $z\to -iz$. We then have

$$I(\alpha)=-\int_{i\infty}^{0} dz\frac{z(z^2-z_F^2)e^{i\alpha z}}{1-(z-\sqrt{1+z^2})^4 e^{2ik_0 dz}\cos^2(\theta/2)},\quad 0<\arg\alpha<\frac{\pi}{2} . \tag{A9}$$

Again, let us digress for a moment to consider the singularities of the integrand of Eq. (A9) for $\mathrm{Re}z,\mathrm{Im}z>0$. Let us examine the function

$$g(z)=1-(z-\sqrt{1+z^2})^4 e^{2ik_0 dz}\cos^2\frac{\theta}{2} . \tag{A10}$$

Defining $z=\mathrm{R}e^{i\phi}$ and $\sqrt{1+z^2}=R'e^{i\phi'}$, then

$$R'=[1+2R^2\cos 2\phi+R^4]^{1/4} \tag{A11a}$$

and

$$\phi'=\frac{1}{2}\arctan\left[\frac{R^2\sin 2\phi}{1+R^2\cos 2\phi}\right] . \tag{A11b}$$

Note, from the form of Eq. (A11b), as $R\to 0$, $\phi'\to 0$ and as $R\to\infty$, $\phi'\to\phi$. In fact, restricting $0\leq\phi\leq\pi/2$, it should be clear that Eq. (A11b) implies $0\leq\phi'\leq\phi\leq\pi/2$. Therefore, $\sqrt{1+z^2}$ always "lags behind" z in the first quadrant of the complex plane of z; $\mathrm{Re}z,\mathrm{Im}z>0$ we always have $0\leq\cos(\phi-\phi')\leq 1$, which means

$$\left|\frac{z-\sqrt{1+z^2}}{z+\sqrt{1+z^2}}\right|^2=\frac{R^2+R'^2-2RR'\cos(\phi-\phi')}{R^2+R'^2+2RR'\cos(\phi-\phi')}\leq 1 ,\quad 0\leq\phi\leq\pi/2 . \tag{A12}$$

Now consider the zeros of Eq. (A10); the zeros of $g(z)$ must satisfy

$$(z-\sqrt{1+z^2})^4 e^{2ik_0 dz}\cos^2\frac{\theta}{2}=1 , \tag{A13a}$$

or equivalently, rearranging the expression and taking the modulus

$$\left|\frac{z-\sqrt{1+z^2}}{z+\sqrt{1+z^2}}\right|^2\left|e^{2ik_0 dz}\cos^2\frac{\theta}{2}\right|=1 . \tag{A13b}$$

Clearly, keeping in mind Eq. (A12), Eq. (A13b) cannot hold unless $\theta=0$ and $z=0$ since otherwise $|e^{2ik_0 dz}\cos^2(\theta/2)|\leq 1$. Thus, $g(z)$ has no zeros except for the case $\theta=0$, $z=0$. Furthermore, setting $\theta=0$ in the integrand of Eq. (A9), and taking the limit as $z\to 0$, we find the finite value $z_F^2/(4-2ik_0 d)$. Hence, we can conclude that the integrand of Eq. (A9) has no poles in the first quadrant of the complex plane.

If we now consider a contour within the first quadrant of the complex plane of z, consisting of the positive imaginary axis, the positive real axis, and a radial part taken infinitely far from the origin, then Eq. (A9) can be equated to an integral along the real axis. Thus, it is now possible to write $I(\alpha)$ as

$$I(\alpha)=\int_0^{\infty} dz\frac{z(z^2-z_F^2)e^{i\alpha z}}{1-(z-\sqrt{1+z^2})^4 e^{2ik_0 dz}\cos^2(\theta/2)},\quad 0<\arg\alpha<\frac{\pi}{2} . \tag{A14}$$

In this way, Eq. (A8) yields

$$j^{(\uparrow)}=-\frac{\hbar k_0^4}{4\pi^2 m}\int_0^\infty dz \frac{z(z-\sqrt{1+z^2})^4(z^2-z_F^2)\sin(2k_0 dz)\sin\theta}{1-2(z-\sqrt{1+z^2})^4\cos(2k_0 dz)\cos^2(\theta/2)+(z-\sqrt{1+z^2})^8\cos^4(\theta/2)} . \quad \text{(A15)}$$

[1]P. Grünberg, R. Schreiber, Y. Pang, M. B. Brodsky, and H. Sowers, Phys. Rev. Lett. **57**, 2442 (1986).

[2]F. Saurenbach, U. Walz, L. Hinchey, P. Grunberg, and W. Zinn, J. Appl. Phys. **63**, 3473 (1988).

[3]F. Nguyen van Dau, A. Fert, P. Etienne, M. N. Baibich, J. M. Brota, J. Chazelas, G. Creuzet, A. Friederich, S. Hadjoudj, H. Hurdequint, J. P. Redoules, and J. Massies, J. Phys. (Paris) Colloq. **49**, C8-1633 (1988).

[4]S. S. P. Parkin, N. More, and K. P. Roche, Phys. Rev. Lett. **64**, 2304 (1990).

[5]J. J. Krebs, P. Lubitz, A. Chaiken, and G. A. Prinz, Phys. Rev. Lett. **63**, 1645 (1989); J. J. Krebs, P. Lubitz, A. Chaiken, and G. A. Prinz, J. Appl. Phys. **67**, 5920 (1990).

[6]M. B. Stearns, C. H. Lee, and Y. Cheng, J. Appl. Phys. **67**, 5925 (1990).

[7]M. E. Brubaker, J. E. Mattson, C. H. Sowers, and S. D. Bader, Appl. Phys. Lett. **58**, 2306 (1991).

[8]S. T. Purcell, M. T. Johnson, N. W. E. McGee, R. Coehoorn, and W. Hoving, Phys. Rev. B **45**, 13 064 (1992).

[9]A. Cebollada, J. L. Martinez, J. M. Gallego, J. J. de Miguel, R. Miranda, S. Ferrer, F. Batallan, G. Fillion, and J. P. Rebouillat, Phys. Rev. B **39**, 9726 (1989).

[10]W. R. Bennett, W. Schwarzacher, and W. F. Egelhoff, Jr., Phys. Rev. Lett. **65**, 3169 (1990).

[11]B. Heinrich, Z. Celinski, J. F. Cochran, W. B. Muir, J. Rudd, Q. M. Zhong, A. S. Arrott, K. Myrtle, and J. Kirschner, Phys. Rev. Lett. **64**, 673 (1990); Z. Celinski and B. Heinrich, J. Magn. Magn. Mater. **99**, L25 (1991).

[12]S. S. P. Parkin, P. Bhodra, and K. P. Roche, Phys. Rev. Lett. **66**, 2152 (1991).

[13]D. M. Edwards, J. Mathon, R. B. Muniz, and M. S. Phan, Phys. Rev. Lett. **67**, 493 (1991).

[14]M. Rührig, R. Schäfer, A. Hubert, R. Mosler, J. A. Wolf, S. Demokritov, and P. Grünberg, Phys. Status Solidi A **125**, 635 (1991).

[15]J. Unguris, R. J. Celotta, and D. T. Pierce, Phys. Rev. Lett. **69**, 1125 (1992).

[16]C. J. Gutierrez, J. J. Krebs, M. E. Filipkowski, and G. A. Prinz, J. Magn. Magn. Mater. (to be published).

[17]J. C. Slonczewski, Phys. Rev. Lett. **67**, 3172 (1991).

[18]J. C. Slonczewski, Phys. Rev. B **39**, 6995 (1989).

[19]See, for example, L. I. Schiff, *Quantum Mechanics,* 3rd ed. (McGraw-Hill, New York, 1968), pp. 101–105.

[20]L. I. Schiff, *Quantum Mechanics* (Ref. 19), pp. 25–27.

[21]V. Korenman, J. L. Murray, and R. E. Prange, Phys. Rev. B **16**, 4032 (1977).

[22]A. Bardasis, D. S. Falk, R. A. Ferrell, M. S. Fullenbaum, R. E. Prange, and D. L. Mills, Phys. Rev. Lett. **14**, 298 (1965).

[23]K. B. Hathaway and J. R. Cullen, J. Magn. Magn. Mater. **104-107**, 1840 (1992).